Supporting Information for

Inactivation of the particulate methane monooxygenase (pMMO) in *Methylococcus capsulatus* (Bath) by acetylene

Minh D. Pham[a,b,c], Ya-Ping Lin[d], Quan Van Vuong[e], Penumaka Nagababu[a], Brian T.-A. Chang[a], Kok Yaoh Ng[a], Chein-Hung Chen[d], Chau-Chung Han[f], Chung-Hsuan Chen[d], Mai Suan Li[e,g], Steve S.-F Yu[a,*], Sunney I. Chan[a,h,i,*]

[a] Institute of Chemistry, Academia Sinica, Taipei 11529, Taiwan; [b] Taiwan International Graduate Program (TIGP), Academia Sinica, Taipei 11529, Taiwan; [c] Department of Chemistry, National Tsing Hua University, Hsinchu 30013, Taiwan; [d] Genomic Research Center, Academia Sinica, Taipei 11529, Taiwan; [e] Institute for Computational Science and Technology, Ho Chi Minh City, Vietnam; [f] Institute of Atomic and Molecular Sciences, Academia Sinica, Taipei 10617, Taiwan; [g] Institute of Physics, Polish Academy of Sciences, 02-668 Warsaw, Poland; [h] Department of Chemistry, National Taiwan University, Taipei 10617, Taiwan; [i] Division of Chemistry and Chemical Engineering, California Institute of Technology, Pasadena, CA 91125, USA

Table of contents

I. Supplementary Figures

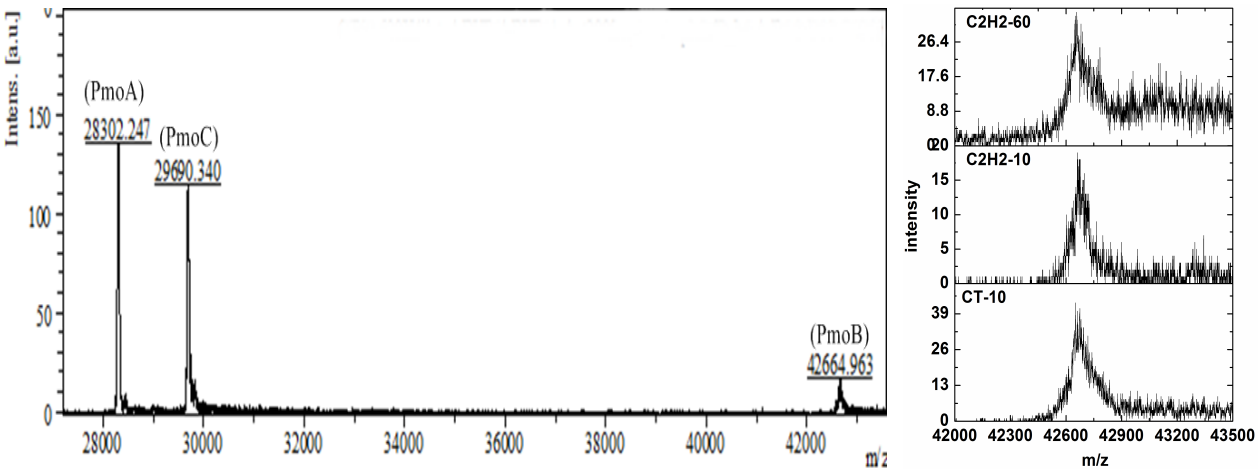

Fig. S1. ***Left panel:*** MALDI-TOF MS analysis of the intact pMMO complex without acetylene treatment; ***Right panel:*** Comparison of the mass peak of the PmoB subunit between untreated-sample (CT-10) and acetylene-treated samples at 10 min (C_2H_2-10) and 60 min (C_2H_2-60).

(A)

```
  1 MHETKQGGEK RFTGAICRCS HRYNSMEVKM AATTIGGAAA AEAPLLDKKW
 51 LTFALAIYTV FYLWVRWYEG VYGWSAGLDS FAPEFETYWM NFLYTEIVLE
101 IVTASILWGY LWKTRDRNLA ALTPREELRR NFTHLVWLVA YAWAIYWGAS
151 YFTEQDGTWH QTIVRDTDFT PSHIIEFYLS YPIYIITGFA AFIYAKTRLP
201 FFAKGISLPY LVLVVGPFMI LPNVGLNEWG HTFWFMEELF VAPLHYGFVI
251 FGWLALAVMG TLTQTFYSFA QGGLGQSLCE AVDEGLIAK
```

(B)

```
  1 MSAAQSAVRS HAEAVQVSRT IDWMALFVVF FVIVGSYHIH AMLTMGDWDF
 51 WSDWKDRRLW VTVTPIVLVT FPAAVQSYLW ERYRLPWGAT VCVLGLLLGE
101 WINRYFNFWG WTYFPINFVF PASLVPGAII LDTVLMLSGS YLFTAIVGAM
151 GWGLIFYPGN WPIIAPLHVP VENNGMLMSI ADIQGYNYVR TGTPEYIRMV
201 EKGTLRTFGK DVAPVSAFFS AFMSILIYFM WHFIGRWFSN ERFLQST
```

Fig. S2. The LC-MS/MS analysis of the in-gel chymotryptic digestion of the "~27 kDa" and "~23 kDa" bands excised from the SDS-PAGE gel of the pMMO complex. The matched peptides are shown in red. (**A**) The sequence coverage of the "~27 kDa" protein band or PmoC is 65%, and (**B**) 74% for the "~23 kDa" protein band or PmoA.

PmoB	1 MKTIKDRIAK WSAIGLLSAV AATAFYAPSA SAHGEKSQAA FMRMRTIHWY 51 DLSWSKEKVK INETVEIKGK FHVFEGWPET VDEPDVAFLN VGMPGPVFIR 101 KESYIGGQLV PRSVRLEIGK TYDFRVVLKA RRPGDWHVHT MMNVQGGGPI 151 IGPGKWITVE GSMSEFRNPV TTLTGQTVDL ENYNEGNTYF WHAFWFAIGV 201 AWIGYWSRRP IFIPRLLMVD AGRADELVSA TDRKVAMGFL AATILIVVMA 251 MSSANSKYPI TIPLQAGTMR GMKPLELPAP TVSVKVEDAT YRVPGRAMRM 301 KLTITNHGNS PIRLGEFYTA SVRFLDSDVY KDTTGYPEDL LAEDGLSVSD 351 NSPLAPGETR TVDVTASDAA WEVYRLSDII YDPDSRFAGL LFFFDATGNR 401 QVVQIDAPLI PSFM
PmoC	1 MHETKQGGEK RFTGAICRCS HRYNSMEVKM AATTIGGAAA AEAPLLDKKW 51 LTFALAIYTV FYLWVRWYEG VYGWSAGLDS FAPEFETYWM NFLYTEIVLE 101 IVTASILWGY LWKTRDRNLA ALTPREELRR NFTHLVWLVA YAWAIYWGAS 151 YFTEQDGTWH QTIVRDTDFT PSHIIEFYLS YPIYIITGFA AFIYAKTRLP 201 FFAKGISLPY LVLVVGPFMI LPNVGLNEWG HTFWFMEELF VAPLHYGFVI 251 FGWLALAVMG TLTQTFYSFA QGGLGQSLCE AVDEGLIAK
PmoA	1 MSAAQSAVRS HAEAVQVSRT IDWMALFVVF FVIVGSYHIH AMLTMGDWDF 51 WSDWKDRRLW VTVTPIVLVT FPAAVQSYLW ERYRLPWGAT VCVLGLLLGE 101 WINRYFNFWG WTYFPINFVF PASLVPGAII LDTVLMLSGS YLFTAIVGAM 151 GWGLIFYPGN WPIIAPLHVP VENNGMLMSI ADIQGYNYVR TGTPEYIRMV 201 EKGTLRTFGK DVAPVSAFFS AFMSILIYFM WHFIGRWFSN ERFLQST

Fig. S3. Sequence coverage in the LC-MS/MS analysis of the acetylene (HCCH)-treated pMMO complex (PmoA: green; PmoB: blue; and PmoC: purple). The amino acids that are not covered in the experiment are highlighted in red text.

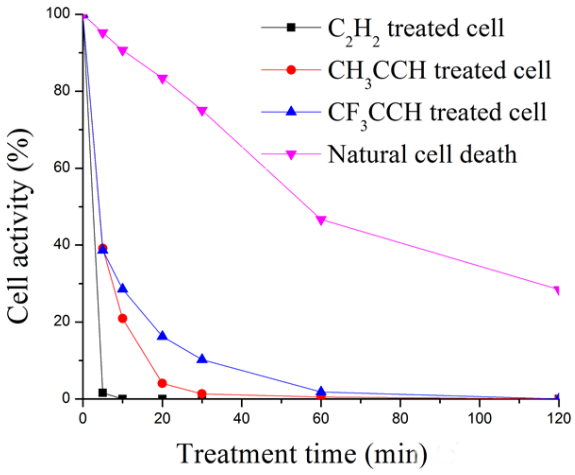

Fig. S4. Kinetics of inhibition of pMMO by three inhibitors based on whole cell assays. Cells of *M. capsulatus* (Bath) cultured under 30 μM Cu^{2+} are treated with HCCH, CH_3CCH, and CF_3CCH in separate experiments, and the activity of the pMMO is assayed by propylene oxidation at various times by GC-MS.

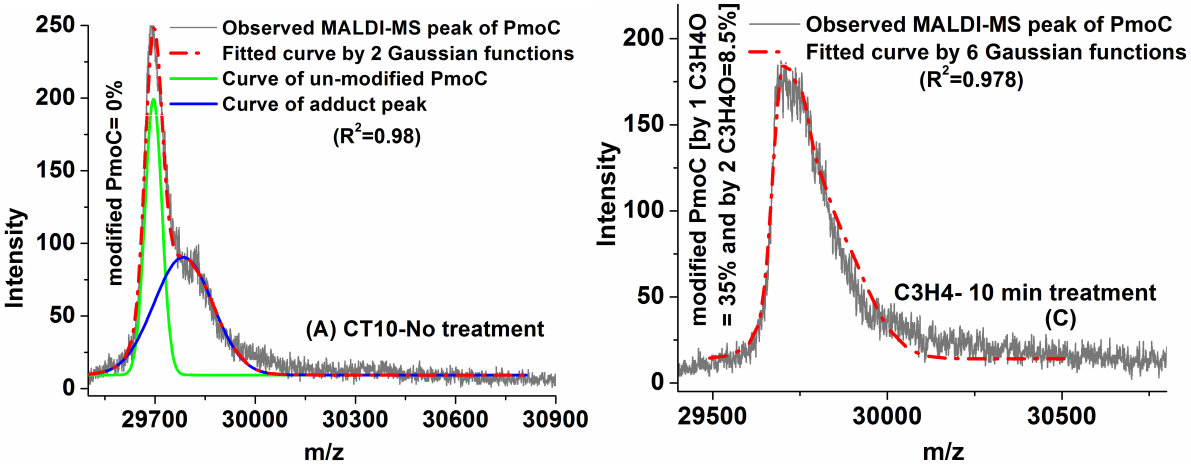

Fig. S5. Quantitation of the PmoC mass shift data. Fitting of the mass signals of the PmoC subunit from untreated and CH_3CCH-treated pMMO (C_3H_4-treatment) to a sum of contributions from chemically modified and unmodified species. The MALDI-TOF MS signal of PmoC after 10 min-treatment with C_3H_4 best fits 6 Gaussian functions representing signals from unmodified PmoC, PmoC modified with 1 methyl ketene, and PmoC modified with 2 methyl ketenes. For details of the fitting and calculation of the percentage of each chemical modification, see **Materials and Methods.**

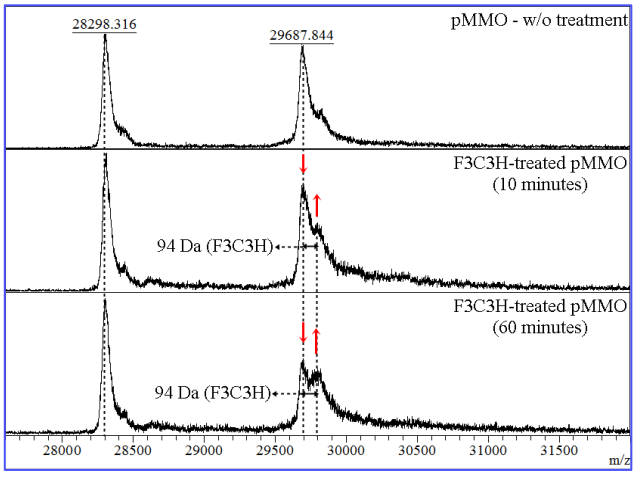

Fig. S6. MALDI-TOF MS analysis of the CF_3CCH-treated pMMO and untreated samples in time-course experiments. Whole cells were treated with and without CF_3CCH (F_3C_3H-treated pMMO) in separate experiments at two time points (10 and 60 min), as described in the kinetic study (Figure S4). Cells were then broken and the pMMO was purified. The MALDI-MS was performed directly on the intact purified pMMO proteins (see **Materials and Methods** section for details).

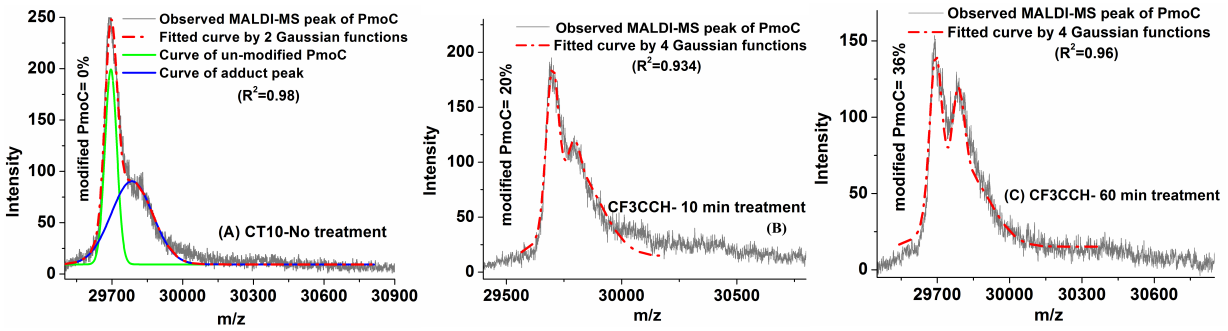

Fig. S7. Quantitation of the PmoC mass shift data. Fitting of the mass signals of the PmoC subunits from the untreated and CF_3CCH-treated pMMO to a sum of contributions from chemically modified and unmodified species. The percentage of chemically modified PmoC subunit was determined from the relative contribution of the two species to the composite PmoC mass signal in each case: *panel* **A**, untreated pMMO; *panel* **B**, CF_3CCH-treated pMMO (10 min); and (*panel* **C**), CF_3CCH-treated pMMO (60 min). Two Gaussian functions and four Gaussian functions were used to fit the unmodified PmoC subunit and the alkyne-modified PmoC subunit, respectively. For details of the fitting, see **Materials and Methods.**

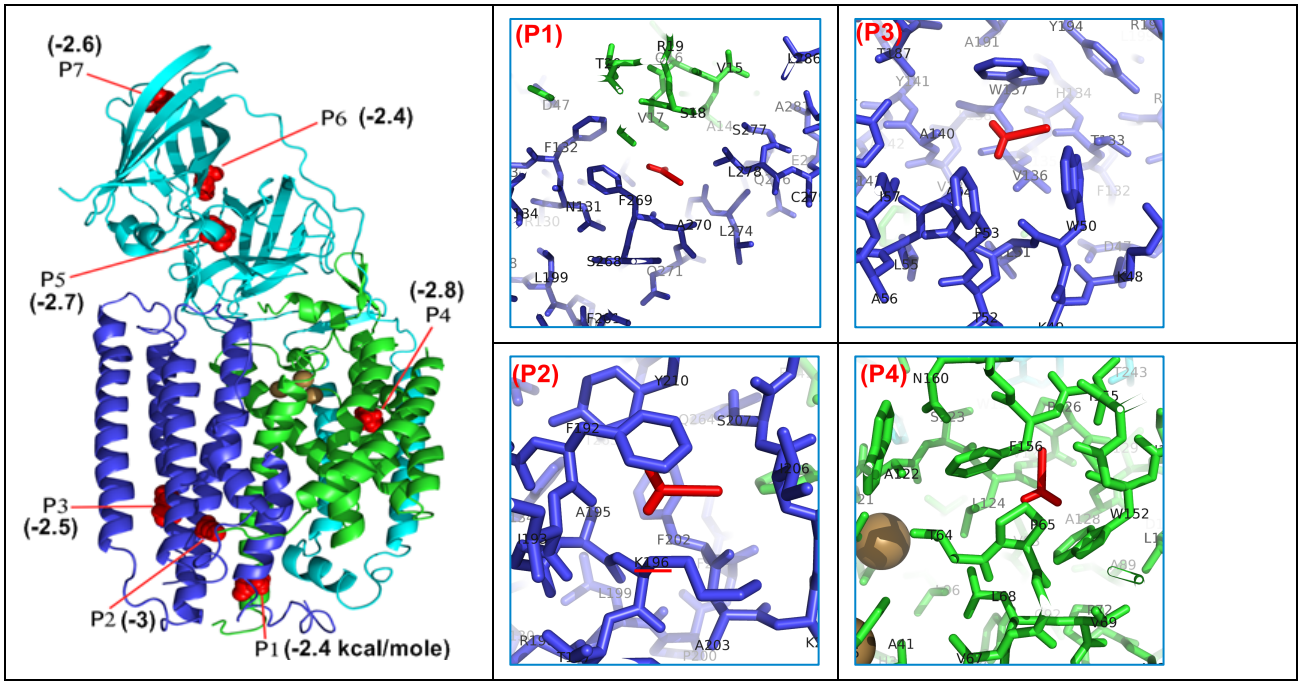

Fig. S8. **Molecular docking of ketene to the revised crystal structure of pMMO (accession number 3RGB).** There are 7 affinity binding sites of ketene denoted from P1 to P7. The surrounding residues of four affinity sites within the transmembrane domain are presented in the right. Predicted binding energy (kcal/mole) of ketene to each position is provided in parentheses, showing the highest binding affinity for P2. K196 is underlined in (P2) showing its proximity to the affinity binding site number 2 or P2, which is also in the cluster of two other sites P1 and P3. The putative tricopper cluster (D site) is highlighted in

brown spheres. Crystal structure of pMMO from *M. capsulatus* used in this study is reproduced from PDB (accession number 3RGB).

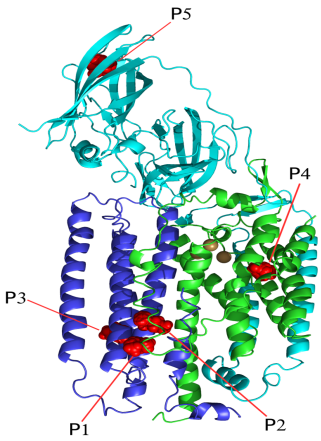

	CH_4	C_2H_6	C_3H_8	C_4H_{10}	C_5H_{12}	C_2H_2
P1	−1.5	−2.9	−3.8	−3.8	×	−2.9
P2	−1.3	−2.5	−3.3	−3.8	−4.3	−2.4
P3	−1.2	−2.2	−2.9	−3.5	−4.0	−2.3
P4	−1.2	−2.3	−3.1	−3.7	−4.2	−2.3
P5	−1.1	−2.1	−3.0	−3.7	−4.0	−2.2

Fig. S9. Predicted binding sites of *n*-alkanes (C1-C5) as well as the suicide-substrate acetylene by molecular dockings in the crystal structure of pMMO (accession number 1YEW) and the corresponding binding energies (kcal/mole). × indicates no binding affinity.

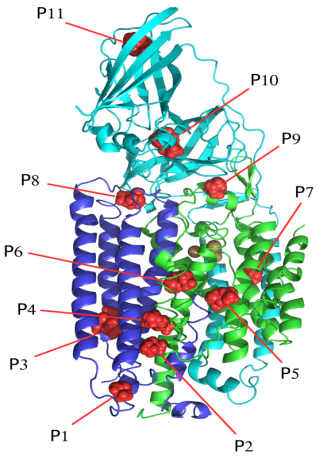

	Methanol	Ethanol	Propan-2-ol	Butan-2-ol	Pentan-2-ol
P1	−1.9	−2.6	−3.0	×	×
P2	×	−2.8	×3.0	×	×
P3	×	×	×	−3.6	−3.8
P4	−2.0	−3.0	×	×	−3.9
P5	×	×	−3.2	−3.6	−4.0
P6	×	×	−3.2	−3.5	−3.8
P7	−1.9	−2.7	−3.4	−4.1	−4.3
P8	−2.0	−2.7	−3.0	−3.4	×
P9	−1.9	×	×	−3.4	-3.8
P10	−1.9	−2.6	−3.1	−3.5	-3.9
P11	-2.1	−3.0	−3.7	−4.5	-4.5

Fig. S10. Predicted binding sites of some alcohols in pMMO and the corresponding binding energies (kcal/mole). × indicates no binding affinity.

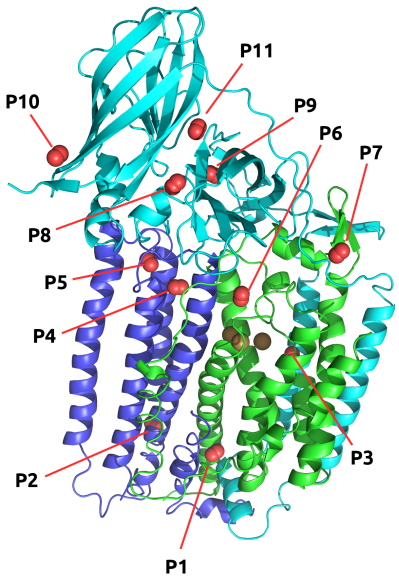

Positions	Binding energy (units)
P1	−2.1
P2	−2.0
P3	−2.2
P4	−2.1
P5	−2.0
P6	−2.1
P7	−2.0
P8	−2.1
P9	−2.4
P10	−2.0
P11	−2.1

Fig. S11. Predicted binding sites of dioxygen in pMMO and the corresponding binding energies (kcal/mole).

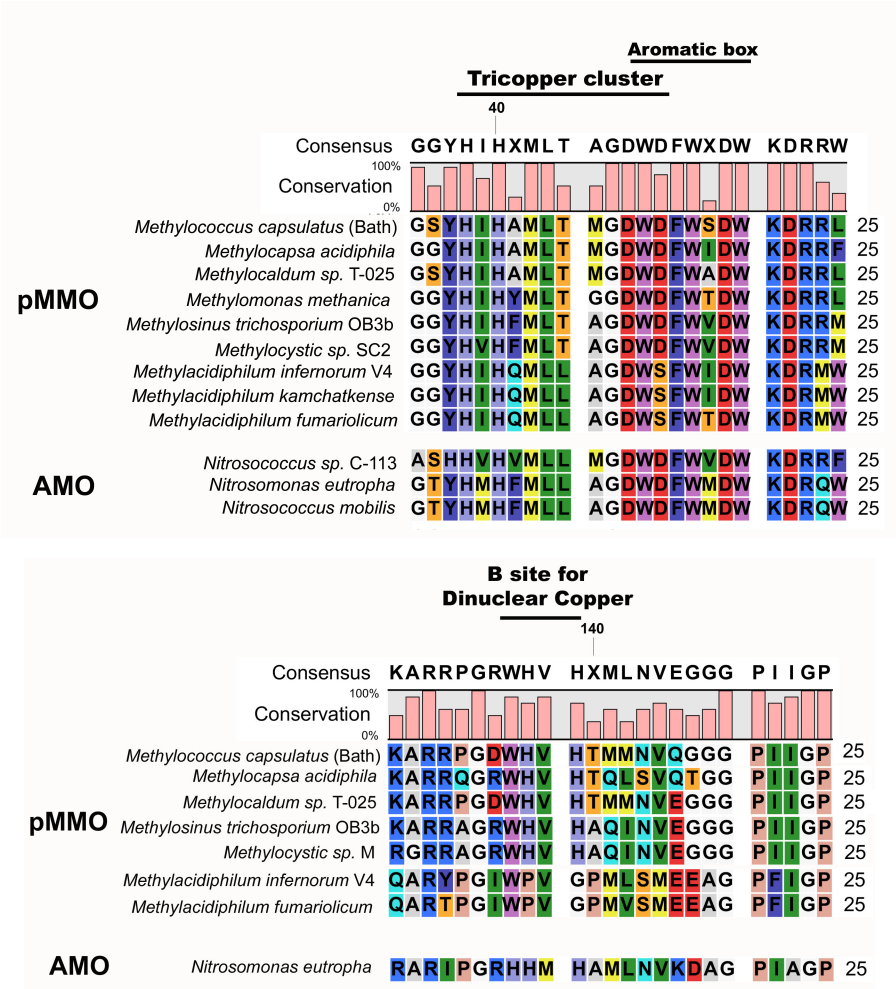

Fig. S12. ***Upper panel:*** Sequence alignments of the PmoA subunits in the region containing both the copper-binding residues for the tricopper cluster and the substrate-binding pocket (aromatic box) in pMMOs from proteobacterial methanotrophs and extremely acidophilic methanotrophs. A similar putative copper-binding peptide domain has been identified in several ammonia monooxygenases. ***Lower panel:*** Sequence alignments of the PmoB subunits in the region containing the copper-binding residues for the dinuclear B site in pMMOs from proteobacterial methanotrophs and the corresponding region in the PmoB subunits of extremely acidophilic methanotrophs. These binding residues are not conserved between the two types of methanotrophs. However, a similar copper-binding peptide domain has been identified in the AMO from *Nitrosomonas eutrophaea.*

Fig. S13. Whole sequence alignments between AMO and pMMO for subunit A (PmoA *vs* AmoA) and subunit C (PmoC vs AmoC) using ClustalW.

Whole sequence alignment of PmoA *vs* AmoA

```
>_ Pmo-A                                                247 aa vs.

>_ Amo-A                                                276 aa

scoring matrix: , gap penalties: -12/-2

44.6% identity;         Global alignment score: 849
```

```
                    10        20        30        40        50
Pmo-A   MSAAQS-----AVRSHAEAVQVSRTIDWMALFVVFFVIVGSYHIHAMLTMGDWDFWSDWK
        ::  ..     :..   :::..:: :: . . .....::.::.: ::  :::::: :::
Amo-A   MSIFRTEEILKAAKMPPEAVHMSRLIDAVYFPILIILLVGTYHMHFMLLAGDWDFWMDWK
                10        20        30        40        50        60

           60        70        80        90       100       110
Pmo-A   DRRLWVTVTPIVLVTFPAAVQSYLWERYRLPWGATVCVLGLLLGEWINRYFNFWGWTYFP
        ::. : .:::::: .:. .:.. :::  :: :.:::.::. ::.:::..::..:. :...:
Amo-A   DRQWWPVVTPIVGITYCSAIMYYLWVNYRQPFGATLCVVCLLIGEWLTRYWGFYWWSHYP
                70        80        90       100       110       120

         120       130       140       150       160       170
Pmo-A   INFVFPASLVPGAIILDTVLMLSGSYLFTAIVGAMGWGLIFYPGNWPIIAPLHVPVEYNG
        :::: :. ..:::..:: .:.:. ..: ::.::.  .::.::::::::..: :.:.  .:
Amo-A   INFVTPGIMLPGALMLDFTLYLTRNWLVTALVGGGFFGLLFYPGNWPIFGPTHLPIVVEG
                130       140       150       160       170       180

         180       190       200       210       220       230
Pmo-A   MLMSIADIQGYNYVRTGTPEYIRMVEKGTLRTFGKDVAPVSAFFSAFMSILIYFMWHFIG
         :.:.:: .:. ::::::::::.: .:.:.:::::  .. ..:::::::.:.:.. .: ..:
Amo-A   TLLSMADYMGHLYVRTGTPEYVRHIEQGSLRTFGGHTTVIAAFFSAFVSMLMFTVWWYLG
                190       200       210       220       230       240

                                  240
Pmo-A   RW----------------------FSNERFLQST-
        .                         :..: : ..
Amo-A   KVYCTAFFYVKGKRGRIVHRNDVTAFGEEGFPEGIK
                250       260       270
```

Whole sequence alignment of PmoC *vs* AmoC

```
>_ Pmo-C                                                    289 aa vs.

>_ Amo-C                                                    271 aa

scoring matrix: , gap penalties: -12/-2

40.5% identity;        Global alignment score: 768
```

```
                10        20        30        40        50
PmoC   MHETKQGGEKRFTGAICRCSHRYNSMEVKMAATTIGGAAAAEAPLLDKKWLTFAL-AIYT
       :  :  :     :..    : :  .: . .                :.:.  :.. ..
AmoC   M-ATTLG-----TSSASSVSSRGYDMSLWY----------------DSKFYKFGMITMLL
                   10        20                        30

       60        70        80        90       100       110
PmoC   VFYLWVRWYEGVYGWSAGLDSFAPEFETYWMNFLYTEIVLEIVTASILWGYLWKTRD--R
       :  .:: ::.  ...: :.::. :::.  ::..  .....  . : . ::.. ::::  .
AmoC   VAIFWV-WYQRYFAYSHGMDSMEPEFDRVWMGLWRVHMAIMPLFALVTWGWILKTRDTKE
       40         50        60        70        80        90

       120       130       140       150       160       170
PmoC   NLAALTPREELRRNFTHLVWLVAYAWAIYWGASYFTEQDGTWHQTIVRDTDFTPSHIIEF
       .:  : :. :..: : ...:: .: ...:::.:.::::..:::.:.:::.::::::.. :
AmoC   QLDNLDPKLEIKRYFYYMMWLGVYIFGVYWGGSFFTEQDASWHQVIIRDTSFTPSHVVMF
       100       110       120       130       140       150

       180       190       200       210       220       230
PmoC   YLSYPIYIITGFAAFIYAKTRLPFFAKGISLPYLVLVVGPFMILPNVGLNEWGHTFWFME
       : :.:.::. : :...:: ::::.:..::::.: .. ..:::::::::::::::.:::::
AmoC   YGSFPMYIVCGVATYLYAMTRLPLFSRGISFPLVMAIAGPLMILPNVGLNEWGHAFWFME
       160       170       180       190       200       210

       240       250       260         270       280
PmoC   ELFVAPLHYGFVIFGWLALAVMGTLTQ--TFYSFAQGGLGQSLCEAVDEGLIAK
       ::: ::::.::::..:: .:   :. .:  : ::     . ..  . . .. :.
AmoC   ELFSAPLHWGFVVLGWAGLFQGGVAAQIITRYSNLTDVVWNNQSKEILNNRIVA
       220       230       240       250       260       270
```

II. Supplementary Tables

Table S1. Predicted molecular masses of the pMMO subunits and the values in Daltons measured by MALDI-TOF MS.

Subunit	Predicted Molecular mass (Average)	Observed Molecular mass (Average)	NCBI reference sequence
PmoB	42 649.000	42 664.663	YP_114234.1
PmoC	29 689.360	29 690.340	YP_114236.1
PmoA	28 294.240	28 302.247	YP_114235.1

Table S2. MS/MS spectra of the identified peptides labeled by ketene (C_2H_2O, +42.0106 Da), methyl ketene (C_3H_4O, +56.0262 Da) and trifluropropyne (F_3C_3H, +94.003 Da). The blue arrows illustrate the b and/or y ions from the fragments of the identified peptides.

<table>
<tr><th>Residue #</th><th>Chemical modification</th><th>MS/MS spectra of identified peptides</th></tr>
<tr><td>K196 (PmoC)</td><td>Ketene (C_2H_2O, + 42.0106 Da)</td><td>
<table>
<tr><th>Query</th><th>Observed</th><th>Mr(expt)</th><th>Mr(calc)</th><th>Delta</th><th>Miss</th><th>Score</th><th>Expect</th><th>Rank</th><th>Peptide</th><th>Modification</th></tr>
<tr><td>690</td><td>437.7614</td><td>873.5082</td><td>873.5072</td><td>1.18</td><td>0</td><td>(21)</td><td>0.0078</td><td>1</td><td>Y.AKTRLPF.F</td><td>+ C2H2O</td></tr>
</table>
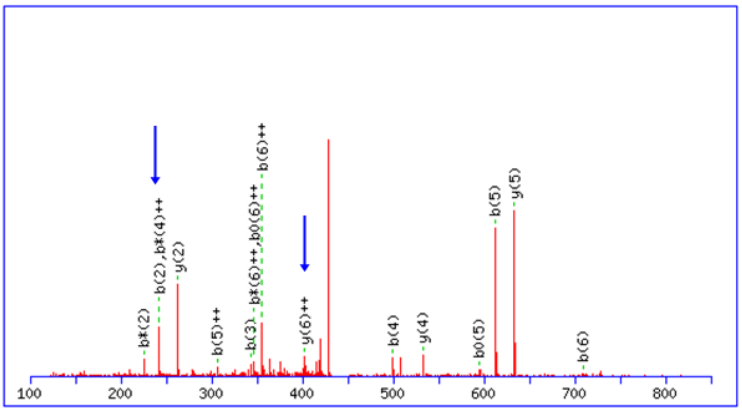

Monoisotopic mass of neutral peptide Mr(calc): 873.5072
Variable modifications:
K2 : C2H2O-KSR (KRS)
Ions Score: 21 Expect: 0.0012
Matches (Bold Red): 16/52 fragment ions using 30 most intense peaks
<table>
<tr><th>#</th><th>b</th><th>b++</th><th>b*</th><th>b*++</th><th>b0</th><th>b0++</th><th>Seq.</th><th>y</th><th>y++</th></tr>
<tr><td>1</td><td>72.0444</td><td>36.5258</td><td></td><td></td><td></td><td></td><td>A</td><td></td><td></td></tr>
<tr><td>2</td><td>242.1499</td><td>121.5786</td><td>225.1234</td><td>113.0653</td><td></td><td></td><td>K</td><td>803.4774</td><td>402.24</td></tr>
<tr><td>3</td><td>343.1976</td><td>172.1024</td><td>326.1710</td><td>163.5892</td><td>325.1870</td><td>163.0972</td><td>T</td><td>633.3719</td><td>317.18</td></tr>
<tr><td>4</td><td>499.2987</td><td>250.1530</td><td>482.2722</td><td>241.6397</td><td>481.2881</td><td>241.1477</td><td>R</td><td>532.3242</td><td>266.66</td></tr>
<tr><td>5</td><td>612.3828</td><td>306.6950</td><td>595.3562</td><td>298.1817</td><td>594.3722</td><td>297.6897</td><td>L</td><td>376.2231</td><td>188.61</td></tr>
<tr><td>6</td><td>709.4355</td><td>355.2214</td><td>692.4090</td><td>346.7081</td><td>691.4250</td><td>346.2161</td><td>P</td><td>263.1390</td><td>132.07</td></tr>
<tr><td>7</td><td></td><td></td><td></td><td></td><td></td><td></td><td>F</td><td>166.0863</td><td>83.54</td></tr>
</table>
</td></tr>
<tr><td>K196 (PmoC)</td><td>Methyl ketene (C_3H_4O, +56.0262 Da)</td><td>
<table>
<tr><td>794</td><td>444.7686</td><td>887.5226</td><td>887.5229</td><td>-0.25</td><td>0</td><td>32</td><td>0.0007</td><td>1</td><td>Y.AKTRLPF.F</td><td>+ C3H4O</td></tr>
</table>
</td></tr>
</table>

<table>
<tr>
<td></td>
<td></td>
<td>
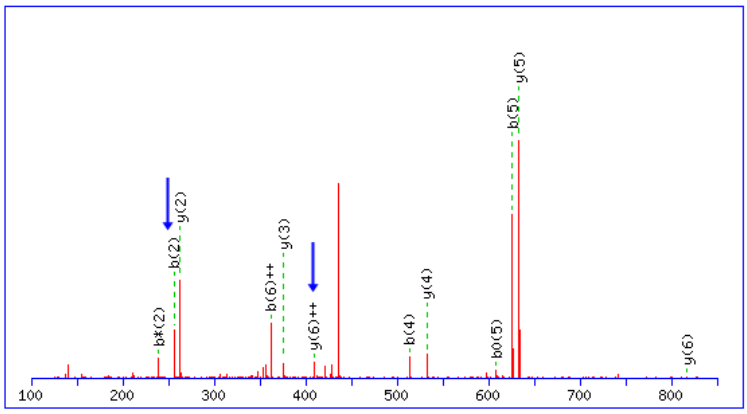

Monoisotopic mass of neutral peptide Mr(calc): 887.5229
Variable modifications:
K2 : C3H4O-KSR (KRS)
Ions Score: 32 Expect: 0.00014
Matches (Bold Red): 12/52 fragment ions using 23 most intense peaks
<table>
<tr><th>#</th><th>b</th><th>b^{++}</th><th>b*</th><th>b*$^{++}$</th><th>b^{0}</th><th>b^{0++}</th><th>Seq.</th><th>y</th><th>y^{++}</th></tr>
<tr><td>1</td><td>72.0444</td><td>36.5258</td><td></td><td></td><td></td><td></td><td>A</td><td></td><td></td></tr>
<tr><td>2</td><td>256.1656</td><td>128.5864</td><td>239.1390</td><td>120.0731</td><td></td><td></td><td>K</td><td>817.4931</td><td>409.2502</td></tr>
<tr><td>3</td><td>357.2132</td><td>179.1103</td><td>340.1867</td><td>170.5970</td><td>339.2027</td><td>170.1050</td><td>T</td><td>633.3719</td><td>317.1896</td></tr>
<tr><td>4</td><td>513.3144</td><td>257.1608</td><td>496.2878</td><td>248.6475</td><td>495.3038</td><td>248.1555</td><td>R</td><td>532.3242</td><td>266.6657</td></tr>
<tr><td>5</td><td>626.3984</td><td>313.7028</td><td>609.3719</td><td>305.1896</td><td>608.3879</td><td>304.6976</td><td>L</td><td>376.2231</td><td>188.6152</td></tr>
<tr><td>6</td><td>723.4512</td><td>362.2292</td><td>706.4246</td><td>353.7160</td><td>705.4406</td><td>353.2239</td><td>P</td><td>263.1390</td><td>132.0731</td></tr>
<tr><td>7</td><td></td><td></td><td></td><td></td><td></td><td></td><td>F</td><td>166.0863</td><td>83.5468</td></tr>
</table>
</td>
</tr>
<tr>
<td>K48
(PmoC)</td>
<td>Methyl ketene (C_3H_4O, +56.0262 Da)</td>
<td>☑ 416 373.2156 744.4166 744.4170 -0.48 1 (19) 0.014 1 L.LDKKW.L + C3H4O</td>
</tr>
</table>

<table>
<tr>
<td></td>
<td></td>
<td>
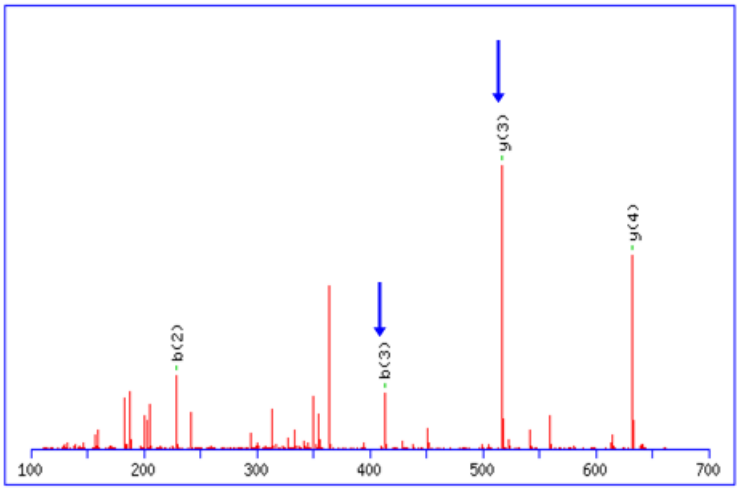

Monoisotopic mass of neutral peptide Mr(calc): 744.4170
Variable modifications:
K3 : C3H4O-KSR (KRS)
Ions Score: 19 Expect: 0.011
Matches (Bold Red): 4/34 fragment ions using 6 most intense peaks
<table>
<tr><th>#</th><th>b</th><th>b^{++}</th><th>b*</th><th>b*$^{++}$</th><th>b^{0}</th><th>b^{0++}</th><th>Seq.</th><th>y</th><th>y^{++}</th></tr>
<tr><td>1</td><td>114.0913</td><td>57.5493</td><td></td><td></td><td></td><td></td><td>L</td><td></td><td></td></tr>
<tr><td>2</td><td>229.1183</td><td>115.0628</td><td></td><td></td><td>211.1077</td><td>106.0575</td><td>D</td><td>632.3402</td><td>316.6</td></tr>
<tr><td>3</td><td>413.2395</td><td>207.1234</td><td>396.2129</td><td>198.6101</td><td>395.2289</td><td>198.1181</td><td>K</td><td>517.3133</td><td>259.1</td></tr>
<tr><td>4</td><td>541.3344</td><td>271.1709</td><td>524.3079</td><td>262.6576</td><td>523.3239</td><td>262.1656</td><td>K</td><td>333.1921</td><td>167.0</td></tr>
<tr><td>5</td><td></td><td></td><td></td><td></td><td></td><td></td><td>W</td><td>205.0972</td><td>103.0</td></tr>
</table>
</td>
</tr>
<tr>
<td>K49
(PmoC)</td>
<td>Methyl ketene (C_3H_4O, +56.0262 Da)</td>
<td>☑ 415 373.2155 744.4164 744.4170 -0.75 1 22 0.0065 1 L.LDKKW.L + C3H4O</td>
</tr>
</table>

		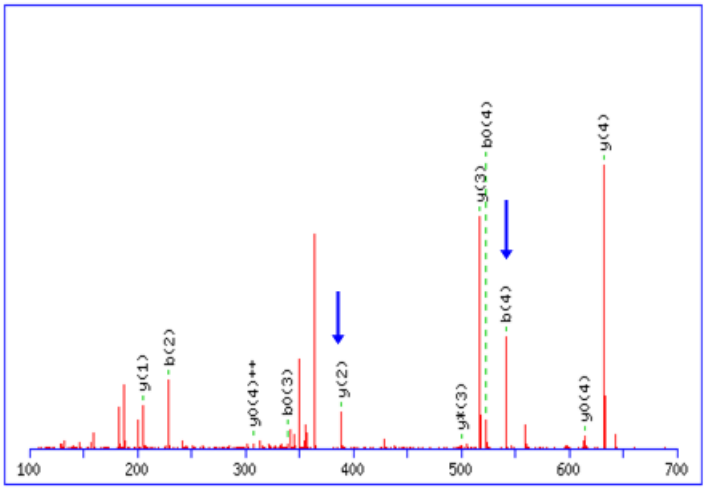 Monoisotopic mass of neutral peptide Mr(calc): 744.4170 Variable modifications: K4 : C3H4O-KSR (KRS) Ions Score: 22 Expect: 0.0052 Matches (Bold Red): 11/34 fragment ions using 31 most intense peaks | # | b | b^{++} | b* | b^{*++} | b^{0} | b^{0++} | Seq. | y | y^{++} | |---|---|---|---|---|---|---|---|---|---| | 1 | 114.0913 | 57.5493 | | | | | L | | | | 2 | **229.1183** | 115.0628 | | | 211.1077 | 106.0575 | D | **632.3402** | 316.6738 | | 3 | 357.2132 | 179.1103 | 340.1867 | 170.5970 | **339.2027** | 170.1050 | K | **517.3133** | 259.1603 | | 4 | **541.3344** | 271.1709 | 524.3079 | 262.6576 | **523.3239** | 262.1656 | K | **389.2183** | 195.1128 | | 5 | | | | | | | W | **205.0972** | 103.0522 |
S277 (PmoC)	Methyl ketene (C_3H_4O, +56.0262 Da)	☑ 4032 1008.0110 2014.0074 2014.0041 1.67 3 64 4.3e-007 1 F.AQGGLGQSLCEAVDEGLIAK.- + C3H40 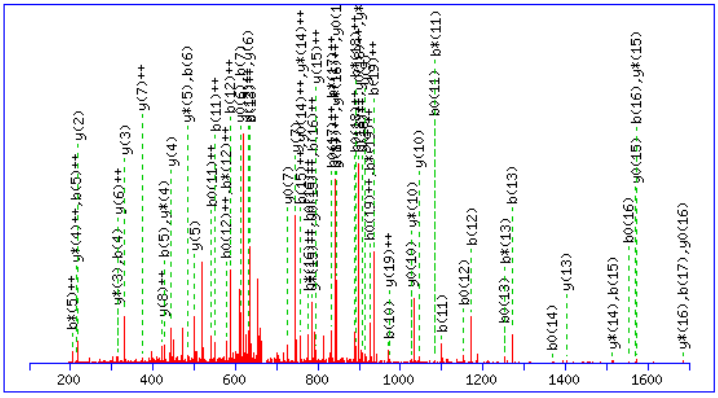

		<table><tr><th>#</th><th>b</th><th>b++</th><th>b*</th><th>b*++</th><th>b0</th><th>b0++</th><th>Seq.</th><th>y</th><th>y++</th><th>y*</th><th>y*++</th><th>y0</th><th>y0++</th><th>#</th></tr><tr><td>1</td><td>72.0444</td><td>36.5258</td><td></td><td></td><td></td><td></td><td>A</td><td></td><td></td><td></td><td></td><td></td><td></td><td>20</td></tr><tr><td>2</td><td>200.1030</td><td>100.5551</td><td>183.0764</td><td>92.0418</td><td></td><td></td><td>Q</td><td>1943.9743</td><td>972.4908</td><td>1926.9477</td><td>963.9775</td><td>1925.9637</td><td>963.4855</td><td>19</td></tr><tr><td>3</td><td>257.1244</td><td>129.0659</td><td>240.0979</td><td>120.5526</td><td></td><td></td><td>G</td><td>1815.9157</td><td>908.4615</td><td>1798.8891</td><td>899.9482</td><td>1797.9051</td><td>899.4562</td><td>18</td></tr><tr><td>4</td><td>314.1459</td><td>157.5766</td><td>297.1193</td><td>149.0633</td><td></td><td></td><td>G</td><td>1758.8942</td><td>879.9508</td><td>1741.8677</td><td>871.4375</td><td>1740.8837</td><td>870.9455</td><td>17</td></tr><tr><td>5</td><td>427.2300</td><td>214.1186</td><td>410.2034</td><td>205.6053</td><td></td><td></td><td>L</td><td>1701.8728</td><td>851.4400</td><td>1684.8462</td><td>842.9267</td><td>1683.8622</td><td>842.4347</td><td>16</td></tr><tr><td>6</td><td>484.2514</td><td>242.6293</td><td>467.2249</td><td>234.1161</td><td></td><td></td><td>G</td><td>1588.7887</td><td>794.8980</td><td>1571.7622</td><td>786.3847</td><td>1570.7781</td><td>785.8927</td><td>15</td></tr><tr><td>7</td><td>612.3100</td><td>306.6586</td><td>595.2835</td><td>298.1454</td><td></td><td></td><td>Q</td><td>1531.7672</td><td>766.3873</td><td>1514.7407</td><td>757.8740</td><td>1513.7567</td><td>757.3820</td><td>14</td></tr><tr><td>8</td><td>755.3682</td><td>378.1878</td><td>738.3417</td><td>369.6745</td><td>737.3577</td><td>369.1825</td><td>S</td><td>1403.7087</td><td>702.3580</td><td>1386.6821</td><td>693.8447</td><td>1385.6981</td><td>693.3527</td><td>13</td></tr><tr><td>9</td><td>868.4523</td><td>434.7298</td><td>851.4258</td><td>426.2165</td><td>850.4417</td><td>425.7245</td><td>L</td><td>1260.6504</td><td>630.8288</td><td>1243.6239</td><td>622.3156</td><td>1242.6399</td><td>621.8236</td><td>12</td></tr><tr><td>10</td><td>971.4615</td><td>486.2344</td><td>954.4349</td><td>477.7211</td><td>953.4509</td><td>477.2291</td><td>C</td><td>1147.5664</td><td>574.2868</td><td>1130.5398</td><td>565.7735</td><td>1129.5558</td><td>565.2815</td><td>11</td></tr><tr><td>11</td><td>1100.5041</td><td>550.7557</td><td>1083.4775</td><td>542.2424</td><td>1082.4935</td><td>541.7504</td><td>E</td><td>1044.5572</td><td>522.7822</td><td>1027.5306</td><td>514.2689</td><td>1026.5466</td><td>513.7769</td><td>10</td></tr><tr><td>12</td><td>1171.5412</td><td>586.2742</td><td>1154.5147</td><td>577.7610</td><td>1153.5306</td><td>577.2690</td><td>A</td><td>915.5146</td><td>458.2609</td><td>898.4880</td><td>449.7477</td><td>897.5040</td><td>449.2556</td><td>9</td></tr><tr><td>13</td><td>1270.6096</td><td>635.8084</td><td>1253.5831</td><td>627.2952</td><td>1252.5991</td><td>626.8032</td><td>V</td><td>844.4775</td><td>422.7424</td><td>827.4509</td><td>414.2291</td><td>826.4669</td><td>413.7371</td><td>8</td></tr><tr><td>14</td><td>1385.6366</td><td>693.3219</td><td>1368.6100</td><td>684.8086</td><td>1367.6260</td><td>684.3166</td><td>D</td><td>745.4090</td><td>373.2082</td><td>728.3825</td><td>364.6949</td><td>727.3985</td><td>364.2029</td><td>7</td></tr><tr><td>15</td><td>1514.6792</td><td>757.8432</td><td>1497.6526</td><td>749.3299</td><td>1496.6686</td><td>748.8379</td><td>E</td><td>630.3821</td><td>315.6947</td><td>613.3556</td><td>307.1814</td><td>612.3715</td><td>306.6894</td><td>6</td></tr><tr><td>16</td><td>1571.7006</td><td>786.3539</td><td>1554.6741</td><td>777.8407</td><td>1553.6900</td><td>777.3487</td><td>G</td><td>501.3395</td><td>251.1734</td><td>484.3130</td><td>242.6601</td><td></td><td></td><td>5</td></tr><tr><td>17</td><td>1684.7847</td><td>842.8960</td><td>1667.7581</td><td>834.3827</td><td>1666.7741</td><td>833.8907</td><td>L</td><td>444.3180</td><td>222.6627</td><td>427.2915</td><td>214.1494</td><td></td><td></td><td>4</td></tr><tr><td>18</td><td>1797.8687</td><td>899.4380</td><td>1780.8422</td><td>890.9247</td><td>1779.8582</td><td>890.4327</td><td>I</td><td>331.2340</td><td>166.1206</td><td>314.2074</td><td>157.6074</td><td></td><td></td><td>3</td></tr><tr><td>19</td><td>1868.9059</td><td>934.9566</td><td>1851.8793</td><td>926.4433</td><td>1850.8953</td><td>925.9513</td><td>A</td><td>218.1499</td><td>109.5786</td><td>201.1234</td><td>101.0653</td><td></td><td></td><td>2</td></tr><tr><td>20</td><td></td><td></td><td></td><td></td><td></td><td></td><td>K</td><td>147.1128</td><td>74.0600</td><td>130.0863</td><td>65.5468</td><td></td><td></td><td>1</td></tr></table>
C279 (PmoC)	Trifluoro-propyne (F_3C_3H, +94.003Da)	☑ 7272 813.8868 1625.7590 1625.7582 0.51 2 87 3.1e-009 1 L.GQSLCEAVDEGLIAK.- + C3F3H 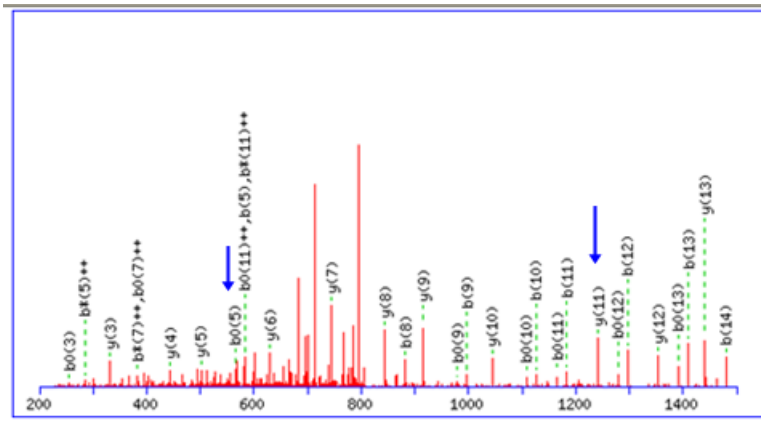 Monoisotopic mass of neutral peptide Mr(calc): 1625.7582 Variable modifications: C5 : C3F3H-KSRCH (CHKRS) Ions Score: 87 Expect: 3.1e-009 Matches (Bold Red): 31/152 fragment ions using 41 most intense peaks <table><tr><th>#</th><th>b</th><th>b++</th><th>b*</th><th>b*++</th><th>b0</th><th>b0++</th><th>Seq.</th><th>y</th></tr><tr><td>1</td><td>58.0287</td><td>29.5180</td><td></td><td></td><td></td><td></td><td>G</td><td></td></tr><tr><td>2</td><td>186.0873</td><td>93.5473</td><td>169.0608</td><td>85.0340</td><td></td><td></td><td>Q</td><td>1569.7441</td></tr><tr><td>3</td><td>273.1193</td><td>137.0633</td><td>256.0928</td><td>128.5500</td><td>255.1088</td><td>128.0580</td><td>S</td><td>1441.6855</td></tr><tr><td>4</td><td>386.2034</td><td>193.6053</td><td>369.1769</td><td>185.0921</td><td>368.1928</td><td>184.6001</td><td>L</td><td>1354.6535</td></tr><tr><td>5</td><td>583.2156</td><td>292.1115</td><td>566.1891</td><td>283.5982</td><td>565.2051</td><td>283.1062</td><td>C</td><td>1241.5694</td></tr><tr><td>6</td><td>712.2582</td><td>356.6328</td><td>695.2317</td><td>348.1195</td><td>694.2477</td><td>347.6275</td><td>E</td><td>1044.5572</td></tr><tr><td>7</td><td>783.2953</td><td>392.1513</td><td>766.2688</td><td>383.6380</td><td>765.2848</td><td>383.1460</td><td>A</td><td>915.5146</td></tr><tr><td>8</td><td>882.3638</td><td>441.6855</td><td>865.3372</td><td>433.1722</td><td>864.3532</td><td>432.6802</td><td>V</td><td>844.4775</td></tr><tr><td>9</td><td>997.3907</td><td>499.1990</td><td>980.3641</td><td>490.6857</td><td>979.3801</td><td>490.1937</td><td>D</td><td>745.4090</td></tr><tr><td>10</td><td>1126.4333</td><td>563.7203</td><td>1109.4067</td><td>555.2070</td><td>1108.4227</td><td>554.7150</td><td>E</td><td>630.3821</td></tr><tr><td>11</td><td>1183.4548</td><td>592.2310</td><td>1166.4282</td><td>583.7177</td><td>1165.4442</td><td>583.2257</td><td>G</td><td>501.3395</td></tr><tr><td>12</td><td>1296.5388</td><td>648.7730</td><td>1279.5123</td><td>640.2598</td><td>1278.5283</td><td>639.7678</td><td>L</td><td>444.3180</td></tr><tr><td>13</td><td>1409.6229</td><td>705.3151</td><td>1392.5963</td><td>696.8018</td><td>1391.6123</td><td>696.3098</td><td>I</td><td>331.2340</td></tr><tr><td>14</td><td>1480.6600</td><td>740.8336</td><td>1463.6334</td><td>732.3204</td><td>1462.6494</td><td>731.8284</td><td>A</td><td>218.1499</td></tr><tr><td>15</td><td></td><td></td><td></td><td></td><td></td><td></td><td>K</td><td>147.1128</td></tr></table>

III. Oxidation of HCCH, CH_3CCH, and C_6H_5CCH mediated by a model trinuclear copper complex.

If the oxidation of hydrocarbons by pMMO is mediated by the putative tricopper cluster at site D of the enzyme, as has been implicated by a broad range of biochemical/biophysical studies on the enzyme [1, 2] as well as oxidation of methane and other hydrocarbons recently demonstrated for biomimics of the tricopper cluster [3, 4], then the same tricopper complex should be able to oxidize the suicide substrates HCCH and CH_3CCH to their corresponding ketene derivatives. To confirm this chemistry, we have compared the oxidation of the two suicide substrates with the hydrocarbon substrates of pMMO mediated by the $[Cu^ICu^ICu^I(\textbf{7-Ethppz})]^{1+}$ tricopper complex, where **7-Ethppz** stands for the ligand 3,3'-(1,4-diazepane-1,4-diyl)bis(1-(4-ethylhomopiperazin-1-yl)propan-2-ol) [5]. Recently, Chan and coworkers have demonstrated that the related $[Cu^ICu^ICu^I(\textbf{7-N-Etppz})]^{1+}$ complex, where **7-N-Etppz** stands for the ligand 3,3'-(1,4-diazepane-1,4-diyl)bis[1-(4-ethylpiperazine-1-yl) propan-2-ol], is capable of catalyzing the efficient oxidation of methane and many other straight-chain hydrocarbons from C2-C6 at room temperature, when the complex is activated by O_2 or H_2O_2 [3, 4].

For HCCH and CH_3CCH, we have confirmed that they are indeed converted into ketene products by the model tricopper complex. Products of the oxidation reactions are analyzed by GC-MS as shown in Figure SIII.1 and Figure SIII.2. Although there is no ketene intermediate observed directly by GC-MS, the compounds identified are products of the reactions between the expected ketene intermediate with oxygen and water. This is not surprising as the ketene intermediates are very reactive species, which will quickly react with O_2 or H_2O within the reaction buffer. For instance: (i) ketene reacts with O_2 to form CO_2 and formaldehyde (HCHO); and (ii) the methyl ketene reacts with O_2 to form CO_2 and acetaldehyde (CH_3CHO), or with H_2O to give acetic acid (CH_3COOH) [6-9]. All these products are identified by GC-MS.

To bolster our understanding of the mechanism of the oxidation of HCCH and CH_3CCH mediated by the model tricoppper complex, we have also employed ethynyl-benzene (C_6H_5CCH, or C_8H_6) as a substrate to take advantage of its well-known ketene chemistry [8]. The addition of an "O-atom" across the triple bond of this alkyne will promote cyclization to yield the benzofuran and acetophenone. Indeed, the benzofuran is observed. In addition, there are also other products coming from the reactions of the oxidation product of ethylnyl-benzene intermediate with O_2 and H_2O. As a control, we have observed no reaction between O_2 and this alkyne without the tricopper catalyst, indicating that the

formation of the ketene derivative is indeed mediated by the tricopper cluster at room temperature.

A proposed mechanism for the oxidation of alkynes catalyzed by the $[Cu^{I}Cu^{I}Cu^{I}(\mathbf{7\text{-}Ethppz})]^{1+}$ complex upon activation by H_2O_2 is given in Figure SIII.3.

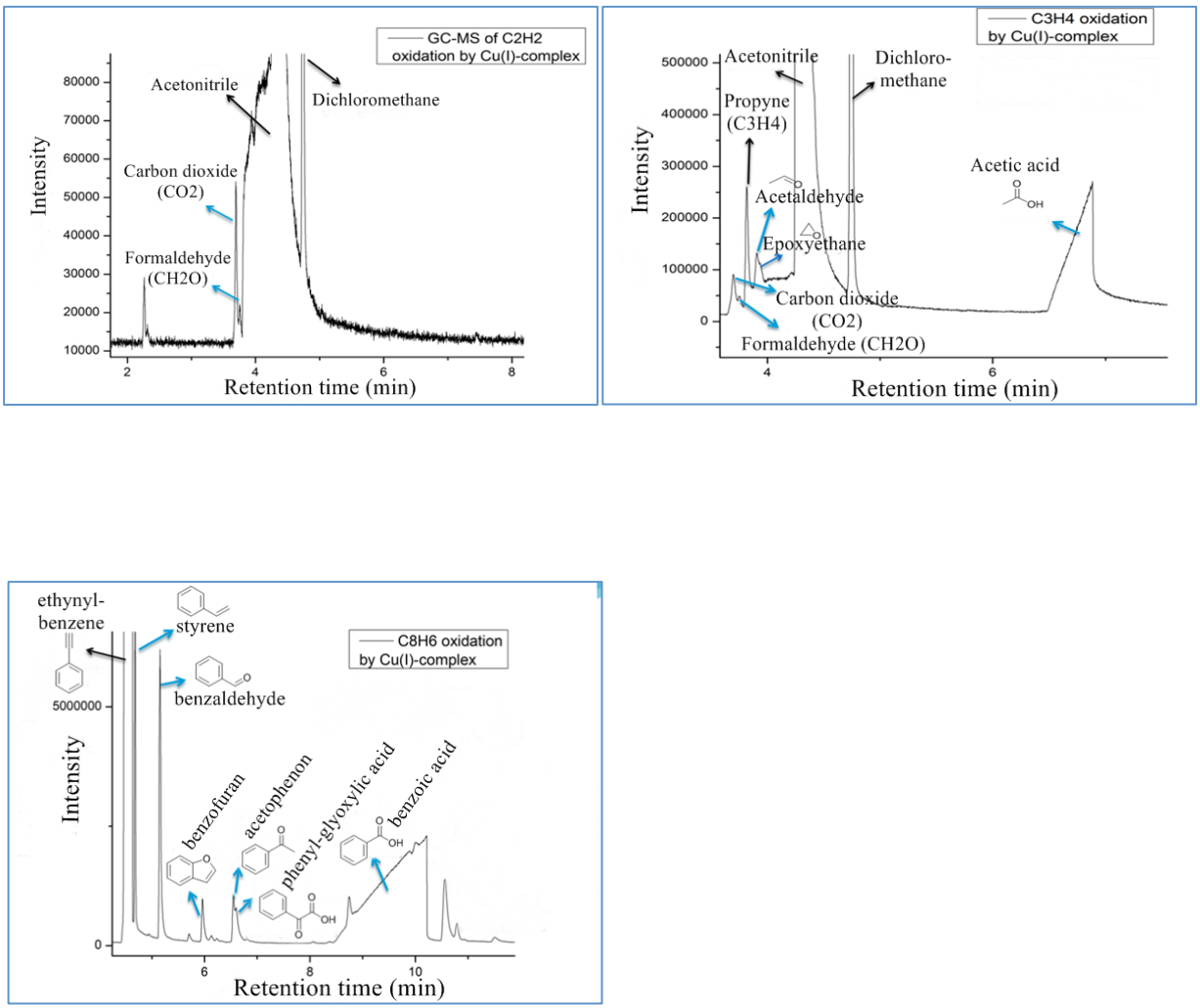

Fig SIII.1. GC-MS analysis of the oxidation of alkynes catalyzed by $[Cu^{I}Cu^{I}Cu^{I}(\mathbf{7\text{-}Ethppz})]^{1+}$ complexes mediated by H_2O_2. The black and blue arrows highlight peaks of the solvent and the products that are formed by the reactions, respectively.

+ ***MS spectrum of the products of ethynyl-benzene (C_8H_6) oxidation***

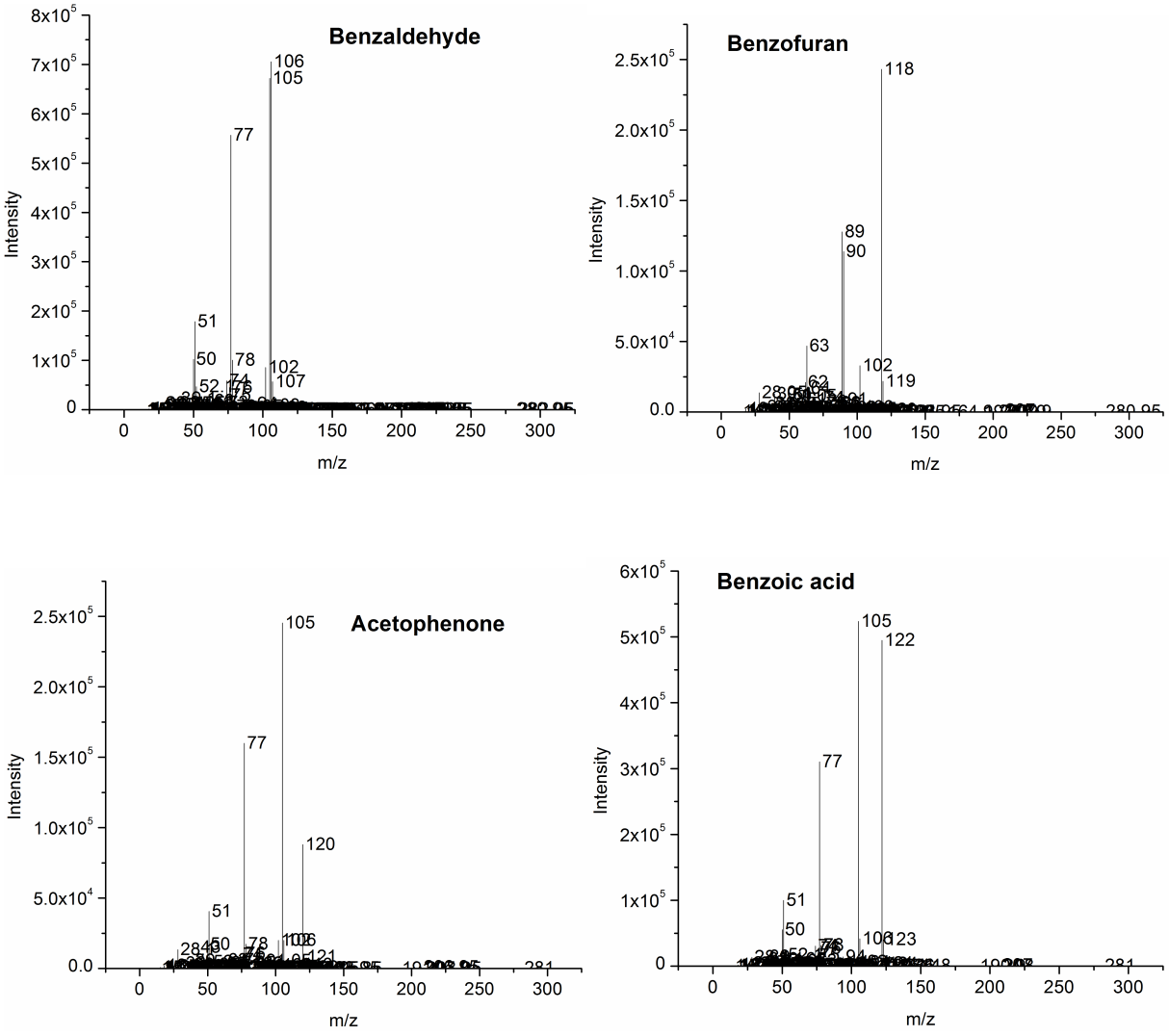

+ ***MS spectrum of the products of CH_3CCH oxidation***

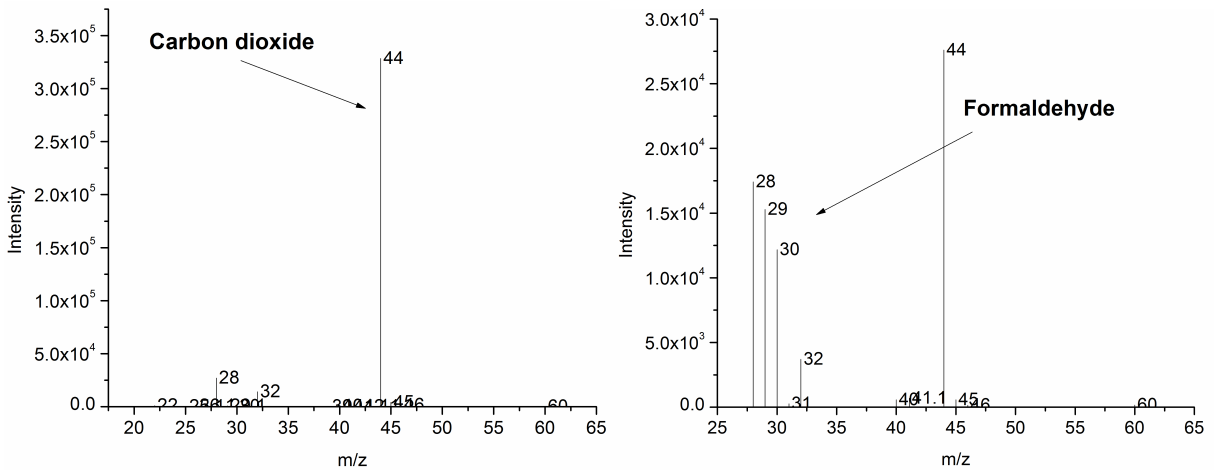

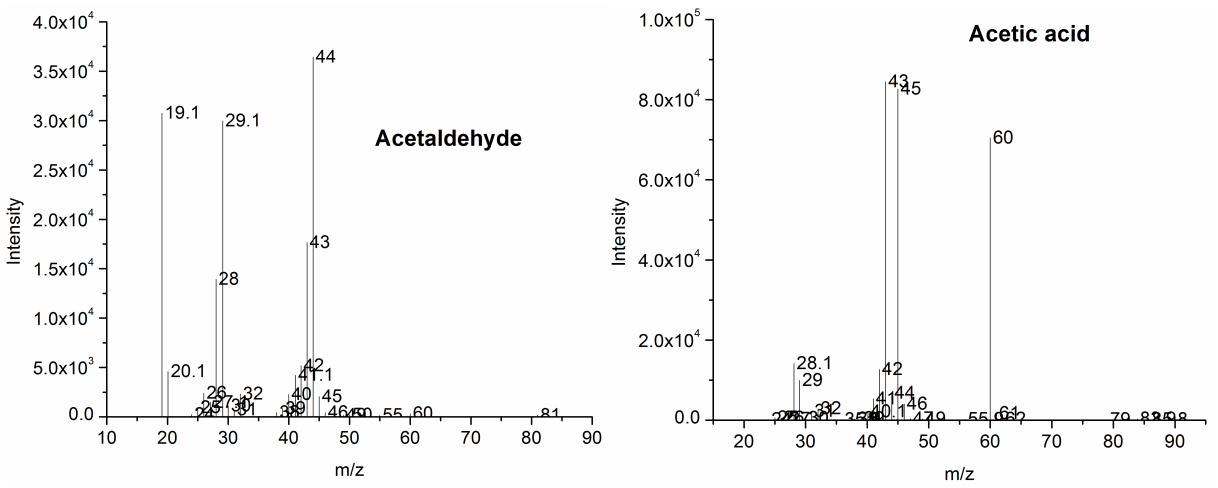

+ *MS spectrum of the products of HCCH oxidation*

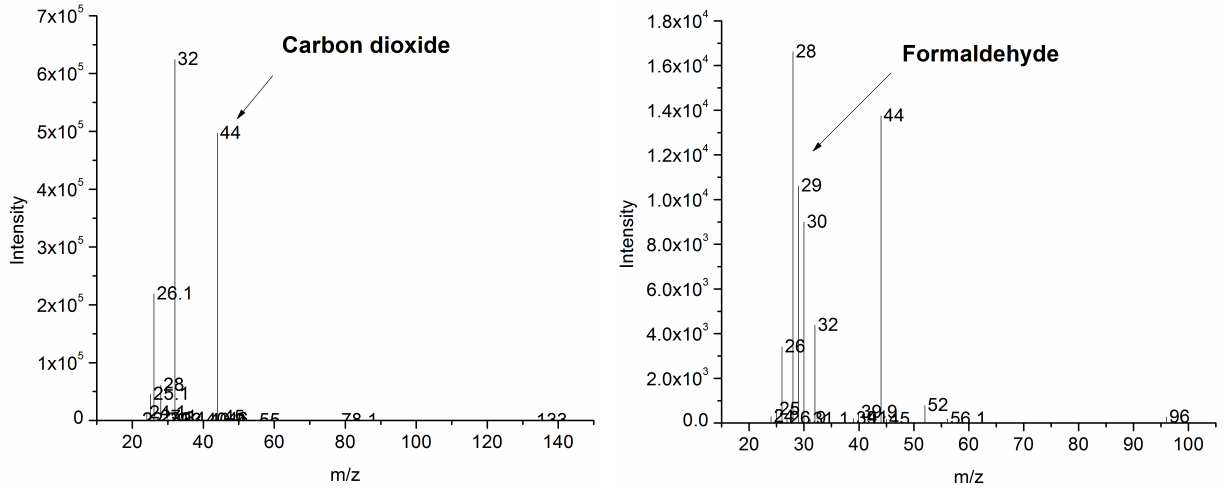

Fig SIII.2. Mass spectrum of products identified from the oxidation of alkynes catalyzed by $[Cu^{I}Cu^{I}Cu^{I}(\mathbf{7\text{-}Ethppz})]^{1+}$ complexes mediated by H_2O_2.

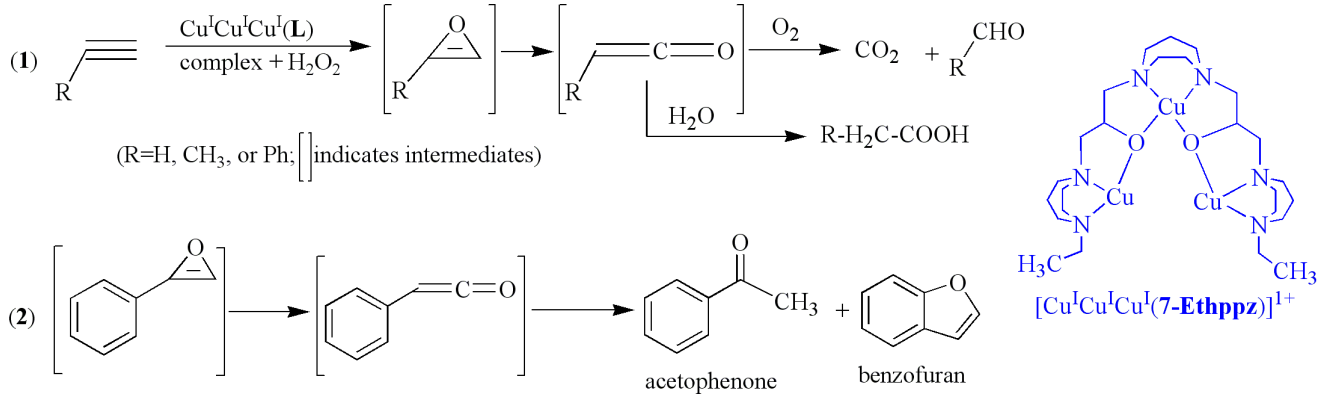

Fig SIII.3. A proposed mechanism for the oxidation of alkynes catalyzed by the $[Cu^ICu^ICu^I$(**7-Ethppz**)$]^{1+}$ complex upon activation by H_2O_2. All reactions are conducted at room temperature, and the products are analyzed by GC-MS. Reaction (1) applies to all three alkynes: HCCH, CH_3CCH, and ethylnyl-benzene (C_6H_5CCH). Reaction (2) is applicable to ethylnyl-benzene only. The inorganic complex to the right represents structure of the $[Cu^ICu^ICu^I$(**7-Ethppz**)$]^{1+}$ tricopper cluster selected for the study.

References

[1] S.I. Chan, S.S.-F. Yu, Controlled oxidation of hydrocarbons by the membrane-bound methane monooxygenase: The case for a tricopper cluster, Acc. Chem. Res., 41 (2008) 969-979.

[2] S.I. Chan, K.H.C. Chen, S.S.F. Yu, C.L. Chen, S.S.J. Kuo, Toward delineating the structure and function of the particulate methane monooxygenase from methanotrophic bacteria, Biochemistry, 43 (2004) 4421-4430.

[3] S.I. Chan, Y.-J. Lu, P. Nagababu, S. Maji, M.-C. Hung, M.M. Lee, I.-J. Hsu, M. Pham Dinh, J.C.-H. Lai, K.Y. Ng, S. Ramalingam, S.S.-F. Yu, M.K. Chan, Efficient oxidation of methane to methanol by dioxygen mediated by tricopper clusters, Angew. Chem. Int. Ed., 52 (2013) 3731-3735.

[4] P. Nagababu, S.S.-F. Yu, S. Maji, R. Ramu, S.I. Chan, Developing an efficient catalyst for controlled oxidation of small alkanes under ambient conditions, Catal. Sci. Technol.,4 (2014) 930-935.

[5] P. Nagababu, S. Maji, M.P. Kumar, P.P.-Y. Chen, S.S.-F. Yu, S.I. Chan, Efficient room-temperature oxidation of hydrocarbons mediated by tricopper cluster complexes with different ligands, Adv. Syn. Catal. 354 (2012) 3275-3282.

[6] T. T. Tidwell, *Ketenes*; John Wiley & Sons: Hoboken, NJ, 2006.

[7] T.T. Tidwell, Ketene chemistry after 100 years: Ready for a new century, Eur. J. Org. Chem, (2006) 563-576.

[8] Pritzkow, W.; Rao, T. S. S. *J. Prakt. Chem.* 327 (1985) 887-892.

[9] D.H. Paull, A. Weatherwax, T. Lectka, Catalytic, asymmetric reactions of ketenes and ketene enolates, Tetrahedron, 65 (2009) 6771-6803.